Displacement Correction in Fourier Transform Spectroscopy of the Mercury Yellow Doublet

Lukas Kostal

***Abstract*—The fundamental principle behind Fourier transform spectroscopy is derived. A modified Michelson interferometer setup with a motorised flexure for displacing one of the mirrors is explained, together with its limitations, and used to obtain measurements for both the mercury green line and the yellow doublet. A data analysis program is presented which uses the Hg green line as a calibration standard to correct for the non-linearity in the displacement of the mirror and which produces a reconstructed spectrum of the yellow mercury doublet. The central wavelengths for the doublet are determined to be 576.66 ± 0.04nm and 578.78 ± 0.04 nm. Wavelengths of three smaller peaks in the spectrum are also determined and the peaks are shown to correspond to emission lines of argon present in the Hg vapour lamp. Finally the positional dependance of the non-linearity of the displacement is analysed and shown to originate from limitations in the mechanical assembly such as misalignment of axis of rotation.**

I. Introduction

In a Michelson interferometer the EM radiation produced by a source, such as an excited mercury vapour, is split into two beams which propagate through the arms of the interferometer and are then superposed with a phase difference $\Delta\phi$ caused by the optical path difference (OPD). The phase difference can therefore be varied by displacing one of the mirrors which changes the relative length of the arms of the interferometer.

A scan is performed by continuously varying the mirror displacement x while sampling the intensity I of the resultant superposition producing an interferogram. Based on the principles from Fourier optics, a Fourier transformation of the interferogram can be used to reconstruct the spectral intensity distribution of the measured source.

In order to resolve details in the spectrum such as the Hg yellow doublet, the displacement of the mirror has to be accurate and linear to an order of 10^{-8} m or less. This turns out to be rather difficult due to mechanical limitations resulting in a non-linear displacement.

To get around this FT spectrometers use a calibration standard with a stable peak of a known wavelength such as the Hg green line. The light from the calibration source is then measured together with the source being analysed and used for correction of the non-linearity during data analysis.

II. Theory

Consider a one dimensional travelling plane wave with an angular wavenumber $k = \frac{2\pi}{\lambda}$ and an angular frequency ω travelling in the $+z$ direction. The wave will also have an amplitude $E_0(k)$ which depends on the wavenumber and therefore the wavelength.

$$E(z,t) = E_0 e^{i(kz-\omega t+\phi)} \tag{1}$$

Now consider a superposition of two waves each of which has travelled through a different arm of the interferometer. The waves will be of equal wavelength and angular frequency but will have different phases ϕ_1 and ϕ_2.

$$E(z,t) = E_0 e^{i(kz-\omega t)} \left(e^{\phi_1} + e^{\phi_2}\right) \tag{2}$$

By defining a phase difference $\Delta\phi = \phi_1 - \phi_2$ and applying Euler's formula, Eq. (2) can be rewritten in the following form.

$$\begin{aligned} E(z,t) &= E_0 e^{i(kz-\omega t)} \left(1 + e^{i\Delta\phi}\right) \\ &= E_0 e^{i(kz-\omega t)} \left(\cos\Delta\phi + i\sin\Delta\phi\right) \end{aligned} \tag{3}$$

The intensity of a wave is related to its amplitude as $I \propto |E|^2$. Omitting the constants of proportionality, the intensity of a resulting superposition for a given angular wavenumber k and a phase difference $\Delta\phi$ will therefore be.

$$\begin{aligned} I(\Delta\phi, k) &= \hat{I}\left(k\right)\left(\cos\Delta\phi + i\sin\Delta\phi\right)\left(\cos\Delta\phi - i\sin\Delta\phi\right) \\ &= 2\hat{I}\left(k\right)\left(1+\cos\Delta\phi\right) \end{aligned} \tag{4}$$

Where $\hat{I}(k)$ is a spectral intensity which for a plane wave is just the square of the amplitude of the wave.

$$\hat{I}(k) = |E_0 e^{i(kz-\omega t)}|^2 = \left(E_0(k)\right)^2 \tag{5}$$

The angular wavenumber k can be expressed in terms of the wavenumber $\nu = \frac{1}{\lambda}$ as $k = 2\pi\nu$. The phase difference can be related to the wavenumber ν and the OPD Λ as $\Delta\phi = 2\pi\Lambda\nu$. Eqn. (4) can therefore be rewritten as shown below.

$$I(\Lambda,\nu) = 2\hat{I}\left(\nu\right)\left(1+\cos\left(2\pi\Lambda\nu\right)\right) \tag{6}$$

Integrating this expression over all of the possible wavelengths characterised by ν gives an expression for the intensity observed with a polychromatic source as a function of Λ only.

$$\begin{aligned} I(\Lambda) &= 2\int_0^\infty \hat{I}(\nu)\left(1+\cos\left(2\pi\Lambda\nu\right)\right)d\nu \\ &= 2\int_0^\infty \hat{I}(\nu)\cos\left(2\pi\Lambda\nu\right)d\nu + C \end{aligned} \tag{7}$$

Multiplying out the brackets the integral of $\hat{I}(\nu)$ just gives a constant C and it is easy to see that the remaining integral has the form of a Fourier cosine transform $\mathcal{F}_c$ which is a specific case of the more general Fourier transform $\mathcal{F}$.

$$\begin{aligned} I(\Lambda) &= \mathcal{F}_c\left(\hat{I}(\nu)\right) + C \\ \hat{I}(\nu) &= \mathcal{F}_c^{-1}\left(I(\Lambda) - C\right) \end{aligned} \tag{8}$$

The optical path difference can be related to the displacement x of one of the mirrors as $\Lambda = 2nx$, where n is the refractive index of the medium through which the mirror is displaced.

Equation (7) describes the key principle behind Fourier transformation spectroscopy (FTS). It shows that measuring the intensity while varying the displacement x and then taking the inverse Fourier transform of the measured interferogram can be used to reconstruct a spectrum, showing the spectral intensity distribution of the measured source $\hat{I}(\lambda)$.

In practice the constant C is removed during data analysis by first passing the interferogram through an AC coupling filter. The forward FT is used instead of the inverse FT since due to the invertibility properties of FTs they will give the same but reversed spectrum.

III. Experimental Setup

As shown in Fig. 1, a Michelson interferometer is used with a second beam splitter B2 added at the output of B1 [1].

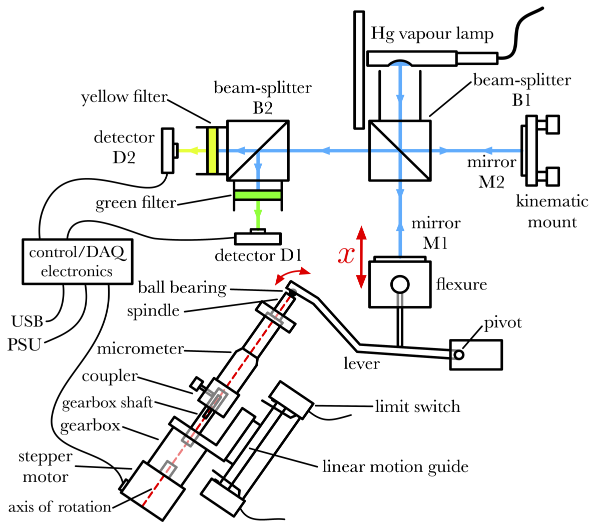

Fig. 1: Modified Michelson interferometer setup for FTS of Hg vapour.

The source used is a UVP pen-ray Hg vapour lamp, powered by an 800 V AC, 50 Hz power supply (PSU) at a current of 20 mA. Detectors D1 and D2 are identical photodiode detectors with an adjustable gain transimpedance amplifier circuit.

The Thorlabs FL543.5-10 green band pass filter is attached to B2 and is used to filter through the Hg green line which is then measured by D1 and used for calibration and correction. For the measurement of the yellow doublet the Thorlabs FB580-10 yellow filter is attached to the other output of B2 which is measured by D2.

The mirror M1 is mounted on a flexure which is displaced by a stepper motor through a series of mechanical reductions. The stepper motor has 200 steps per revolution with micro stepping at 256 μsteps per one step. The motor then rotates a planetary gearbox with a reduction ratio of 100:1 which is coupled to a screw gauge micrometer which moves 1 μm per every 2 rotations. The micrometer then pushes a mechanical lever which displaces the flexure resulting in a reduction ratio of approximately 6.25:1. Based on these parameters the setup is expected to displace the mirror by approximately 1.6×10^{-11} m per every μstep of the stepper motor.

While this setup is capable of displacing the mirror M1 very slowly it also suffers from non-linearity caused by a multitude of mechanical limitations and errors. Since there is no feedback of the final displacement x to the control electronics the non-linearity can not be corrected for real time and so this must be done during the data analysis.

One of the main sources of the non-linearity is the misalignment of the output shaft of the gearbox with the axis of rotation of the micrometer. The coupling between the two will therefore effectively act as a Cardan joint which is known to experience non-linearity described by the equation below [2].

$$\omega_2 = \left(\frac{\cos\beta}{1 - \sin^2\beta\ \cos^2\theta_1} \right) \omega_1 \tag{9}$$

Where β is the angle between the axis of of the output shaft and the micrometer and θ_1 is the angle of rotation of the input shaft given by $\frac{d\theta_1}{dt} = \omega_1$ which gives rise to the non-linear nature of Eq. (9).

Another contributing error occurs at the interface of the flat tip of the micrometer spindle with the ball bearing embedded in the lever. As the lever rotates the angle between the normal to the lever and the axis in which the spindle extends will slowly change. Since the rate at which the lever is rotated depends on the aforementioned angle, it will result in a slowly varying deviation from the linear displacement.

The lever will also undergo thermal expansion which will lead to significant errors when taking long scans with a changing ambient temperature. For the purposes of this experiment this error can be assumed to be negligible since the scans take no longer than 1h and are performed indoors.

Finally the rotating assembly, especially the stepper motor and the planetary gearbox, have a non-zero rotational inertia which results in the overall acceleration of the mirror being limited by the maximum torque of the stepper motor. When a scan is initiated it therefore takes some time (less than 1s) for the motor to reach a constant angular velocity and for the mirror to be displaced at the desired average speed.

IV. Methodology

First a Thorlabs CPS532 laser diode is used as a coherent monochromatic source in place of the Hg lamp to make aligning the mirrors easier. The orientation of the mirror M2 is adjusted using the kinematic mount until circular Haidinger fringes are observed at the detectors.

To determine the null point, the laser is replaced by a source with a narrow coherence length such as a standard LED. The mirror M1 is then moved at the maximum speed of 2×10^5 μsteps s$^-1$ until an interference pattern is observed. The mirror is then moved slowly and the point at which the contrast between the minima and maxima is the greatest is taken to be the approximate null point at which $x = 0$.

The Hg vapour lamp is now mounted in place of the LED and left to reach its operating temperature. A scan is to be carried out for a range of 1×10^8 μsteps or a displacement of approximately 1.46 mm centred about the null point. The mirror is first displaced to a position of $x = -5 \times 10^8$ μsteps and a scan is then initiated up to $x = 5 \times 10^8$ μsteps at a speed of 1×10^5 μsteps s^{-1} and with a sampling frequency of 500Hz. This means that the mirror moves approximately 3.12 nm between sampling.

V. Data Analysis

The analysis of the data obtained from a scan is carried out using a program written in Python. The program along with the collected data, results and additional materials can be found in the following GitHub repository [3].

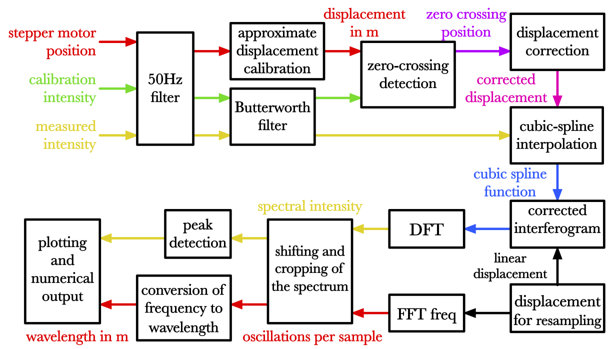

Fig. 2: Flowchart explaining the displacement correction data analysis.

The measured data is first passed through a low-pass finite impulse response filter, which is essentially a moving average. This is done to remove the high frequency interference caused by the intensity of the Hg lamp varying with the 50 Hz supply current. The intensity of the lamp only depends on the amplitude of the supply current, and so it varies at a frequency of 100 Hz. It is found that averaging over each 100 Hz cycle does not remove all of the interference, likely due to the current waveform being not being perfectly symmetric. A moving average is therefore taken over each 50 Hz cycle.

Next the position of the stepper motor is converted from μsteps into m using an approximate calibration constant. Both measured intensities are then passed through a 2nd order high-pass Butterworth filter to remove the DC offset resulting from errors in the alignment of the optical components [1].

The position of the zero-crossings in the interferogram of the green line are now determined by a function which finds consecutive samples for which the sign of the intensity changes. The position of the zero-crossings is then taken to be the x-axis intercept of the line passing through the two points.

The positions of the zero-crossings are passed into a function which calculates a new displacement corrected for non-linearities. This is archived by using the green line as a calibration standard with a wavelength of $\lambda = 546.0750 \pm 0.0001$ nm. The function then looks at the difference between the position of two consecutive zero-crossings $\Delta x'$ and uses it to calculate a wavelength for the green line from the uncorrected spectrum as $\lambda' = \frac{\Delta x'}{4}$. The ratio of the known wavelength and the determined wavelength is then used to correct the displacement as shown below.

$$x_i = \frac{\lambda'}{\lambda}\left(x'_i - x'_j\right) + x_j \tag{10}$$

Where x is the corrected displacement, x' the uncorrected displacement and j is an index such that x'_j is the displacement of the last zero-crossing. This method effectively expands/compresses the uncorrected displacement x' between all of the zero-crossings.

The corrected displacement is used to fit a cubic spline onto the measured intensity. The cubic spline is then resampled at 10^7 samples to give a displacement corrected interferogram.

The spectral intensity $\hat{I}$ is calculated as the absolute value of the discrete Fourier transform (DFT) along with the corresponding frequencies in the units of oscillations per sample. The Fourier spectrum is then shifted, cropped to only include positive frequencies and also normalised. The frequency is converted from oscillations per sample to meters giving a reconstructed spectrum of the Hg yellow doublet.

Finally, the positions of the peaks are determined using the SciPy signal library along with the full width at halve maximum (FWHM) and the standard deviation σ of the peaks. Assuming the peaks to have the form of a Gaussian function the area under the peaks is also calculated and normalised as $A = \frac{a\sigma}{\sqrt{2\pi}}$, where a is the amplitude of the peak. Additionally the position dependance of the non-linearity of the displacement is also analysed as described in the analysis program.

VI. Discussion of Results

The displacement corrected interferogram shown in Fig. 3 shows a clear modulation in the intensity of the bright fringes. Based on the properties of FTs, the distance between the maxima in the modulation envelope is related to the reciprocal of the separation of the wavelengths in the frequency domain.

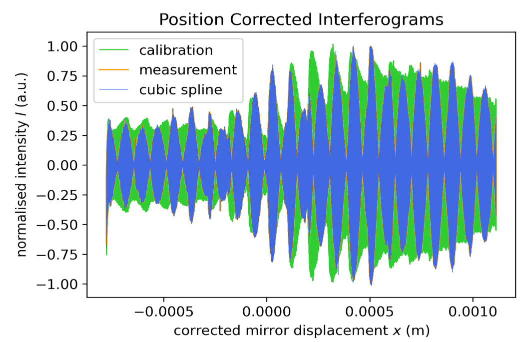

Fig. 3: Interferograms for both the green and yellow lines and the cubic spline.

The interferogram will also include phase errors caused by the waves propagating through air which is a dispersive medium [4]. For a dispersive medium the phase velocity v_p is a function of the wavelength $v_p = v_p(\lambda)$ and so is the refractive index, defined as $n(\lambda) = \frac{v_p}{c}$. This ultimately results in the OPD being not just a function of the displacement x but also the wavelength since it is defined as $\Lambda = 2n(\lambda)x$.

From the zero crossings the average displacement per μstep is determined to be $1.891 \pm 0.003 \times 10^{-11}$ m μstep^{-1} which agrees with the approximate value of 1.6 m μstep^{-1} estimated from the parameters of the mechanical assembly.

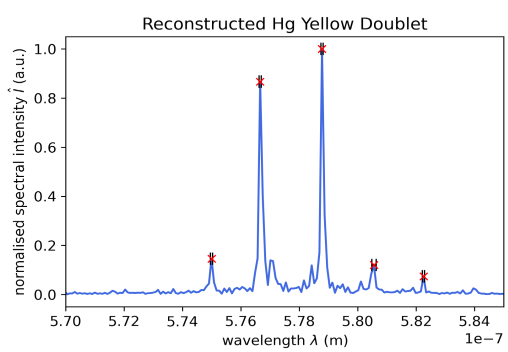

Fig. 4: Displacement corrected spectrum for the Hg yellow doublet.

The two largest peaks in the reconstructed spectrum on Fig. 4 correspond to the measured Hg yellow doublet. The corresponding wavelengths determined from the positions of the peaks are shown in the table below and all agree with the officially accepted values from the NIST database [5].

Numerical Results

Element	Measured λ (nm)	Database λ (nm)
Hg	576.66 ± 0.04	576.961 ± 0.001
Hg	578.78 ± 0.04	578.969 ± 0.005
Ar	575.00 ± 0.04	577.637 ± 0.0008
Ar	580.56 ± 0.08	580.046 ± 0.002
Ar	582.26 ± 0.04	582.60549 ± 0.00007

TABLE I: Wavelengths and associated expected uncertainties obtained from the corrected spectrum compared with values from the NIST database [5].

In addition to the main central peaks, three more smaller peaks can be seen in the reconstructed spectrum. These peaks correspond to the emission lines of Ar which is used as an inert gas buffer inside of the Hg vapour lamp. The wavelengths for these peaks are included in Tab. I and also agree with the officially accepted values.

Since the current supplied to the Hg vapour lamp is approximately 20 mA the splitting of spectral lines caused by the Zeeman effect can be assumed to be negligible [6].

It should also be noted that the width of the peaks will be affected by the Hg vapour pressure inside of the lamp which for the lamp used was significantly lower than the atmospheric pressure. Likewise, the effects of isotopic shifts are not observed in the reconstructed spectrum.

A deviation δx of the uncorrected displacement from a linear displacement can be calculated as $\delta x = x - x'$ and plotted against the corrected displacement as shown in the diagram below.

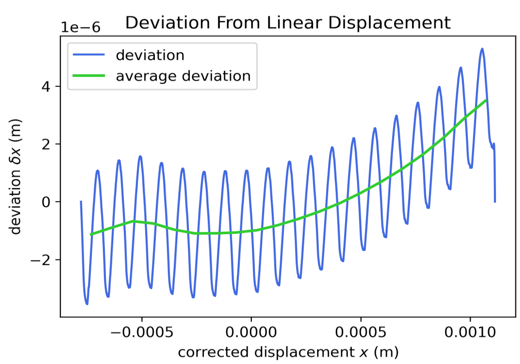

Fig. 5: Plot showing the position dependance of the deviation.

From Fig. 5 it can be seen that at the beginning of the scan the average deviation is negative meaning that the actual displacement of the mirror is lagging behind. This is explained by the finite acceleration of the setup caused by the effects of inertia as discussed in the Experimental Setup section.

The average deviation can also be seen to gradually increase throughout the scan with an overall deviation of 4.62 μm (3sf) and a standard deviation of 1.41 μm (3sf). The slow variation of this error in the displacement as well as the shape of the curve match the description of the error at the interface of the tip of the spindle with the ball bearing which is most likely the source of this non-linearity.

The deviation can also be seen to vary periodically with the position at a relatively high frequency. Using an additional analysis procedure described comments included in the final section of the program, it is determined that the oscillation has an amplitude of 2.65 μm (3sf) and a spatial frequency of $10.0 \pm 0.4\ \mathrm{mm}^{-1}$. For a scan moving at an average speed of 1×10^5 μsteps s^{-1} this corresponds to a frequency of 0.0190 ± 0.0004 Hz. By considering the angular velocity of the stepper motor and the reduction ratio between the motor and the output shaft of the gearbox, the frequency of the rotation of the output shaft is calculated to be 0.0195 Hz (3sf). Since the frequency of the oscillation in the displacement matches with the frequency at which the output shaft of the stepper motor rotates it can be concluded that the periodic variation in the deviation is caused by the misalignment of the gearbox shaft and the micrometer as described by (9).

VII. Conclusion

The wavelengths for the Hg yellow doublet, as well the additional Ar peaks, obtained from the reconstructed spectrum have been shown to agree with the officially accepted values to within the expected uncertainty. It can therefore be concluded that the methods proposed in this paper are capable of calibrating and correcting non-linear displacement resulting from errors in the mechanical assembly.

In the future the measurements should be repeated in a controlled environment and used to characterise the repeatability of the experimental setup and the correction procedure.

The methods presented can be applied to scans of any regions in the visible range of the Hg emission spectrum or even the full spectrum. The data and results for such a scan can be found in the GitHub repository [3].

Ultimately, this setup can be easily modified to measure the spectrum of any source with the addition of suitable calibration standard, such as a stabilised He-Ne laser, giving a versatile FTS setup used widely in research,

References

[1] A. C. David Colling, *Year 2 Interferometry Lab Script*. Imperial College London.

[2] F. Vesali, M. A. Rezvani, and M. Kashfi, “Dynamics of universal joints, its failures and some propositions for practically improving its performance and life expectancy,” *Journal of mechanical science and technology*, vol. 26, no. 8, pp. 2439–2449, 2012.

[3] L. Kostal, “Displacement correction in fourier transform spectroscopy of the mercury yellow doublet github repository,” [Online]. Available: https://github.com/KostalLukas/Displacement-Correction-in-FTS-of-the-Hg-Yellow-Doublet, 2022.

[4] R. Learner and A. Thorne, “Wavelength calibration of fourier-transform emission spectra with applications to fe i,” *JOSA B*, vol. 5, no. 10, pp. 2045–2059, 1988.

[5] A. Kramida, Yu. Ralchenko, J. Reader, and and NIST ASD Team, NIST Atomic Spectra Database (ver. 5.10), [Online]. Available: `https://physics.nist.gov/asd` [2022, November 8]. National Institute of Standards and Technology, Gaithersburg, MD., 2022.

[6] A. C. Melissinos and J. Napolitano, *Experiments in Modern Physics*. Gulf Professional Publishing, 2003.